



Contents lists available at ScienceDirect

Computers and Structures

journal homepage: [www.elsevier.com/locate/compstruc](http://www.elsevier.com/locate/compstruc)

# Identification of the parameters of the Kelvin–Voigt and the Maxwell fractional models, used to modeling of viscoelastic dampers

R. Lewandowski \*, B. Chorążyczewski

Poznan University of Technology, ul. Piotrowo 5, 60-965 Poznan, Poland

## ARTICLE INFO

### Article history:

Received 15 June 2008

Accepted 3 September 2009

Available online xxxx

### Keywords:

Parameters identification  
Fractional rheological models  
Viscoelastic dampers

## ABSTRACT

Fractional models are becoming more and more popular because their ability of describing the behaviour of viscoelastic dampers using a small number of parameters. An important difficulty, connected with these models, is the estimation of model parameters. A family of methods for identification of the parameters of both the Kelvin–Voigt fractional model and the Maxwell fractional model are presented in this paper. Moreover, the equations of hysteresis curves are derived for fractional models. One of the methods presented used the properties of hysteresis curves. The validity and effectiveness of procedures have been tested using artificial and real experimental data.

© 2009 Elsevier Ltd. All rights reserved.

## 1. Introduction

Viscoelastic (VE) dampers have often been used in controlling the vibrations of aircrafts, aerospace and machine structures. Moreover, VE dampers are used in civil engineering to reduce excessive oscillations of building structures due to earthquakes and strong winds. A number of applications of VE dampers in civil engineering are listed in [1]. The VE dampers could be divided broadly into fluid and solid VE dampers. Silicone oil is used to build the fluid dampers while the solid dampers are made of copolymers or glassy substances.

Good understanding of the dynamical behaviour of dampers is required for the analysis of structures supplemented with VE dampers. The dampers behaviour depends mainly on the rheological properties of the viscoelastic material the dampers are made of and some of their geometric parameters. These characteristics depend on the temperature and the frequency of vibration. Temperature changes in dampers can occur due to environmental temperature fluctuations and also on the internal temperature rising due to energy dissipation. A classic shift factor approach is commonly used to capture the effect of temperature changes. Therefore, only the frequency dependence of damper characteristics is considered in this paper.

In a classic approach, the mechanical models consisting of springs and dashpots are used to describe the rheological properties of VE dampers [2–7]. A good description of the VE dampers requires mechanical models consisting of a set of appropriately connected springs and dashpots. In this approach, the dynamic

behaviour of a single damper is described by a set of differential equations (see [5,6]), which considerably complicates the dynamic analysis of structures with dampers because the large set of motion equation must be solved. Moreover, the cumbersome, nonlinear regression procedure, described for example in [8,9], is propose to determine the parameters of the above mentioned models.

The rheological properties of VE dampers are also described using the fractional calculus and the fractional mechanical models. Currently, this approach has received considerable attention and has been used in modeling the rheological behaviour of linear viscoelastic materials [10–15]. The fractional models have an ability to correctly describe the behaviour of viscoelastic material using a small number of model parameters. A single equation is enough to describe the VE damper dynamics, which is an important advantage of the discussed models. In this case, the VE damper equation of motion is the fractional differential equation. The fractional models of VE fluid dampers are proposed in [16,17]. The parameters of the model proposed in [17] are complex numbers which has added to the complexity of the dynamic analysis of structures with VE dampers, especially when the in time domain analysis must be performed. However, fractional models of which the parameters are real numbers are also proposed, for example, in [10,21,22]. The dependence of the above mentioned model parameters on excitation frequency could lead to major complications of analysis of structures with VE dampers in a time domain. Fortunately, efficient time-domain approaches have been proposed recently. The methods, based on Prony series and Biot model, are proposed in papers [4,29,30]. Additionally, the method which used the generalized Maxwell model and the Laguerre polynomial approximation is suggested in [5]. Very recently, seismic analysis of structures with VE dampers modeled by the Kelvin chain and

\* Corresponding author. Tel.: +48 61 6652 472; fax: +48 61 6652 059.  
E-mail address: [roman.lewandowski@put.poznan.pl](mailto:roman.lewandowski@put.poznan.pl) (R. Lewandowski).

the Maxwell ladder is presented in [6]. Moreover, the non-viscous state-space model, described in [31], could be used in this context. The analysis in the frequency domain is possible and presented, for example, in [3].

An important problem, connected with the fractional rheological models, is an estimation of the model parameters from experimental data. In the past, different methods have been tested for the estimation of model parameters from both static and dynamic experiments [4,8,9,16–19,21]. The process of parameter identification is an inverse problem which is overdetermined and can be ill conditioned (see, for example [8,19]) because of noises existing in the experimental data. The mathematical difficulties may be overcome by the regularization method which is described, for example, in [8,18].

It is the aim of this paper to describe a few methods of identification of the parameters of VE dampers. The parameters are estimated using the results obtained from dynamical tests. The fractional rheological models are used to describe the dynamic behaviour of dampers. The Kelvin–Voigt model and the Maxwell model are discussed. Three kinds of identification methods are suggested. Equations of hysteresis curves are derived for both fractional models and some of the properties of these curves are used to develop the first-kind identification procedure. The second- and third-kind identification procedures are based on time series data. Each identification procedure consists of two main steps. In the first step, for the given frequencies of excitation, experimentally obtained data are approximated by simple harmonic functions while model parameters are determined in the second stage of the identification procedure. The results of a typical calculation are presented and discussed.

Three symbols will be used in the paper to describe the damper force. The symbol  $u_e(t)$  denotes the results of experimental measurements,  $\hat{u}(t)$  is the function which is an analytical approximation of experimental results while  $u(t)$  is the solution to the damper equation of motion. The symbols  $q_e(t)$ ,  $\hat{q}(t)$  and  $q(t)$  are used in the same way to describe the damper displacement.

## 2. General explanation of fractional rheological models

Due to their simplicity, the simple rheological models, such as the Kelvin–Voigt model or the Maxwell model, are used very often to describe the dynamic behavior of VE dampers installed on various types of civil structures. For example, the Kelvin–Voigt model is used in papers [2,3,22–24], while the Maxwell model is used in papers [2,3,25–28]. The Kelvin–Voigt model consists of the spring and the dashpot connected in parallel, while the Maxwell model is built from the serially connected spring and dashpot. The discussed simple rheological models have a small number of parameters but do not have enough parameters to accurately capture the frequency dependence of damper parameters. More sophisticated classical rheological models which, however, contain many parameters, can be used to correctly describe the dynamic behavior of VE dampers. Models of this kind are developed in [6,7].

The next group of models used to describe the behaviour of VE dampers are the fractional derivative models. Using the fractional calculus, a number of rheological models, e.g., the fractional Kelvin–Voigt model [32], the fractional Zener model [10,11], the fractional Jeffreys model [12], or the fractional Maxwell model [17] can be developed. It has been proved in [4,15] that the fractional derivative models can better capture the frequency dependent properties of VE dampers. The simple fractional models discussed in [4,13,15] are sufficient to correctly capture the VE dampers properties. These models contain only a few parameters but the dynamic analysis requires knowledge of the fractional calculus.

The simple Kelvin–Voigt model seems to be more appropriate to describe the solid dampers behavior, while the simple Maxwell model is mainly used to describe the liquid dampers behavior. Recently, it has been shown in [6] that both the generalized Kelvin model and the generalized Maxwell model are also useful models of the solid VE damper.

One important problem, considered here and connected with these models, is how to determine model parameters from experimental data in an efficient way. This problem is solved in this Section for the fractional Kelvin–Voigt model and the fractional Maxwell model.

### 2.1. Fractional models equation of motion and the steady state solution to the motion equation

In order to construct the fractional models equation of motion, we introduce the fractional element called the springpot which satisfies the constitutive equation:

$$u(t) = \tilde{c}^\alpha D_t^\alpha q(t) = c D_t^\alpha q(t), \quad (1)$$

where  $c = \tilde{c}^\alpha$  and  $\alpha, 0 < \alpha \leq 1$ , are the springpot parameters and  $D_t^\alpha q(t)$  is the fractional derivative of the order  $\alpha$  with respect to time  $t$ . There are a few definitions of fractional derivatives which coincide under certain conditions. Here, symbols such as  $D_t^\alpha q(t)$  denote the Riemann–Liouville fractional derivatives with the lower limit at  $-\infty$  (see [34]). Some valuable information about fractional calculus can be found in [34].

The springpot element, also known as the Scott–Blair's element (see [33]), is schematically shown in Fig. 1a. The considered element can be understood as an interpolation between the spring element ( $\alpha = 0$ ) and the dashpot element ( $\alpha = 1$ ).

The fractional Kelvin–Voigt model consists of the spring and the springpot connected in parallel, while the fractional Maxwell model is built of the serially connected spring and springpot. These models are shown schematically in Fig. 1b and c, respectively.

The motion equation of the above mentioned fractional Kelvin–Voigt model, obtained in a usual way, is in the following form:

$$u(t) = kq(t) + k\tau^\alpha D_t^\alpha q(t), \quad (2)$$

where  $\tau^\alpha = \tilde{c}^\alpha/k = c/k$ .

The following relationships can be written for the fractional Maxwell model (Fig. 1c)

$$u(t) = kq_1(t), \quad u(t) = \tilde{c}^\alpha D_t^\alpha (q(t) - q_1(t)). \quad (3)$$

Eliminating  $q_1(t)$  from the above relationships, we get the equation in the form:

$$u(t) + \tau^\alpha D_t^\alpha u(t) = k\tau^\alpha D_t^\alpha q(t). \quad (4)$$

It is easy to recognize that both of the considered fractional models have three real and positive value parameters:  $k$ ,  $c$ , and  $\alpha$ .

In the case of a harmonically excited damper, i.e. when

$$q(t) = q_0 \exp(i\lambda t), \quad (5)$$

the steady state solution of the motion equation of both of the fractional models is assumed in the form:

$$u(t) = u_0 \exp(i\lambda t). \quad (6)$$

Taking into account that in our case (see [34, p. 311])

$$D_t^\alpha \exp(i\lambda t) = (i\lambda)^\alpha \exp(i\lambda t), \quad (7)$$

for  $\lambda > 0$ , we obtain the following equations

$$u_0 = k[1 + (i\tau\lambda)^\alpha]q_0, \quad u_0 = k \frac{(i\tau\lambda)^\alpha}{1 + (i\tau\lambda)^\alpha} q_0, \quad (8)$$

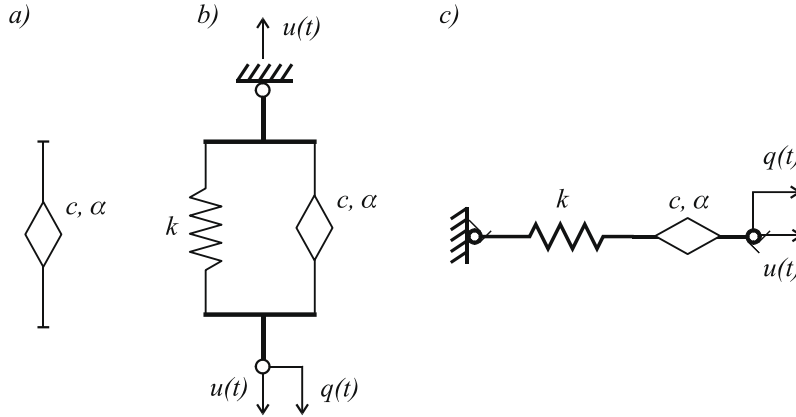


Fig. 1. Diagram of fractional rheological models.

from (2) and (4), respectively. Moreover, after introducing the following formula  $i^\alpha = \cos(\alpha\pi/2) + i\sin(\alpha\pi/2)$ , we can rewrite relationships (8) in the form

$$u_0 = (K' + iK'')q_0 = K'(1 + i\eta)q_0, \quad (9)$$

where  $\eta(\lambda) = K''(\lambda)/K'(\lambda)$  is the loss factor,  $K'(\lambda)$  is the storage modulus and  $K''(\lambda)$  is the loss modulus. These quantities are defined as:

$$K' = k[1 + (\tau\lambda)^\alpha \cos(\alpha\pi/2)], \quad K'' = k(\tau\lambda)^\alpha \sin(\alpha\pi/2), \quad (10)$$

$$\eta = \frac{(\tau\lambda)^\alpha \sin(\alpha\pi/2)}{1 + (\tau\lambda)^\alpha \cos(\alpha\pi/2)}, \quad (11)$$

for the fractional Kelvin–Voigt model and

$$K' = k(\tau\lambda)^\alpha \frac{(\tau\lambda)^\alpha + \cos(\alpha\pi/2)}{1 + (\tau\lambda)^{2\alpha} + 2(\tau\lambda)^\alpha \cos(\alpha\pi/2)}, \quad (12)$$

$$K'' = k(\tau\lambda)^\alpha \frac{\sin(\alpha\pi/2)}{1 + (\tau\lambda)^{2\alpha} + 2(\tau\lambda)^\alpha \cos(\alpha\pi/2)}, \quad (12)$$

$$\eta = \frac{\sin(\alpha\pi/2)}{(\tau\lambda)^\alpha + \cos(\alpha\pi/2)}, \quad (13)$$

for the fractional Maxwell model.

If the classical Kelvin–Voigt model (i.e.  $\alpha = 1$ ) is used as the VE dampers model the above mentioned quantities are given by

$$K'(\lambda) = k, \quad K''(\lambda) = k\tau\lambda, \quad \eta(\lambda) = K''(\lambda)/K'(\lambda) = \tau\lambda \quad (14)$$

while for the classical Maxwell model we have

$$K'(\lambda) = k \frac{\tau^2 \lambda^2}{1 + \tau^2 \lambda^2}, \quad K''(\lambda) = k \frac{\tau\lambda}{1 + \tau^2 \lambda^2}, \quad \eta(\lambda) = \frac{1}{\tau\lambda}. \quad (15)$$

The dependence of the above mentioned model parameters on excitation frequency could significantly complicates in time domain analysis of structures with VE dampers.

According to the classical Kelvin–Voigt model the storage modulus is the constant function of  $\lambda$ , while the loss modulus and the loss factor linearly increases with  $\lambda$ . Behaviour of the fractional Kelvin–Voigt model is substantially different in comparison with the classic Kelvin–Voigt model. The storage modulus is increased significantly when the non-dimensional frequency increases and when the parameter  $\alpha$  decreases. Moreover, the loss modulus and the loss factor decrease for an increasing non-dimensional frequency and the decreasing values of the parameter  $\alpha$ .

The properties of the fractional Maxwell model, for different values of the parameter  $\alpha$  are shown in Figs. 2 and 3. In the figures the non-dimensional frequency is defined as  $\tau\lambda$ . The calculation is made using the value of the  $k$  parameter equal to 1,00,000.0 N/m.

The storage modulus grows with non-dimensional frequency for all values of the parameter  $\alpha$ . However, for  $0 < \tau\lambda < 1$  the function  $K'(\alpha)$  increases for decreasing values of  $\alpha$ . An opposite tendency is evident for  $\tau\lambda > 1$ . The function of the loss modulus could be flat (for instant when  $\alpha = 0.4$ ). Moreover,  $\eta(0) = \text{tg}(\alpha\pi/2)$  which means that the loss factor has a finite value for  $\lambda = 0$ . This is an important difference in comparison with the loss factor function of the classic Maxwell model of which the values approach infinity if  $\lambda$  approaches zero and in comparison with the both versions of the Kelvin–Voigt model for which the loss factor is equal to zero for  $\tau\lambda = 0$ .

According to results presented by Lion in [35] the fractional rheological models fulfill the second law of thermodynamics when values of the storage modulus  $K'(\lambda)$  and the loss modulus  $K''(\lambda)$ , given by formulae (10)–(13), are positive for all possible values of frequency of excitation  $\lambda$ . It can easily be demonstrated that both models fulfill the second law of thermodynamics when  $0 \leq \alpha \leq 1, \tau > 0$  and  $k > 0$ .

If the damper displacement varies harmonically in time and is described using the trigonometric functions, i.e.:

$$q(t) = q_c \cos \lambda t + q_s \sin \lambda t, \quad (16)$$

the steady state solution to the fractional Kelvin–Voigt model equation of motion (2) is given by

$$u(t) = u_c \cos \lambda t + u_s \sin \lambda t, \quad (17)$$

where

$$u_c = \varphi_1 q_c + \varphi_2 q_s, \quad u_s = -\varphi_2 q_c + \varphi_1 q_s, \quad (18)$$

$$\varphi_1 = k + c\lambda^\alpha \cos(\alpha\pi/2), \quad \varphi_2 = c\lambda^\alpha \sin(\alpha\pi/2). \quad (19)$$

The steady state solution to the equation of motion (4) of the fractional Maxwell model is also given by (16) and (17) and the coefficients  $q_c, q_s, u_c$  and  $u_s$  are interrelated in the following way:

$$q_c = \phi_1 u_c - \phi_2 u_s, \quad q_s = \phi_2 u_c + \phi_1 u_s, \quad (20)$$

where

$$\phi_1 = \frac{1}{k(\tau\lambda)^\alpha} \left[ (\tau\lambda)^\alpha + \cos \frac{\alpha\pi}{2} \right], \quad \phi_2 = \frac{1}{k(\tau\lambda)^\alpha} \sin \frac{\alpha\pi}{2}. \quad (21)$$

## 2.2. Hysteresis loops of the damper models

The equation of the hysteresis loops of the fractional Kelvin–Voigt model could be derived if the damper’s kinematical excitation is given by

$$q(t) = q_0 \sin \lambda t. \quad (22)$$

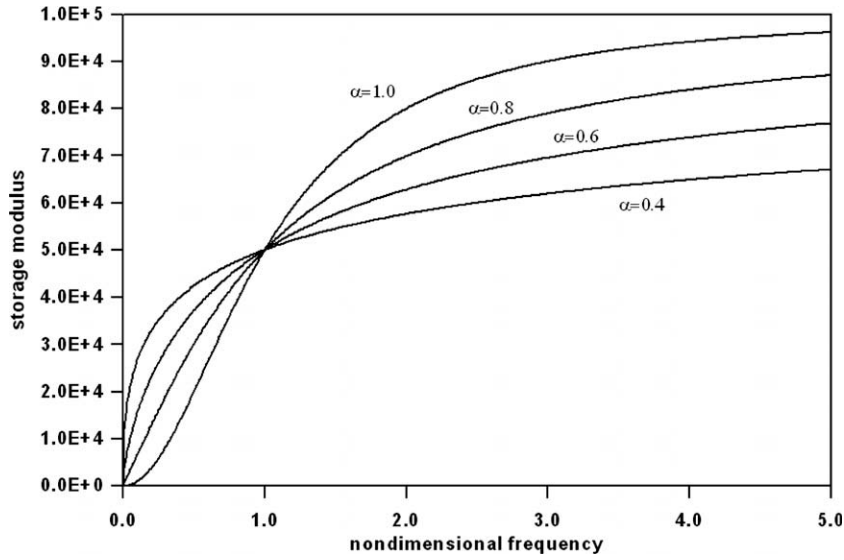


Fig. 2. The storage modulus of the fractional Maxwell model for different values of  $\alpha$  parameter.

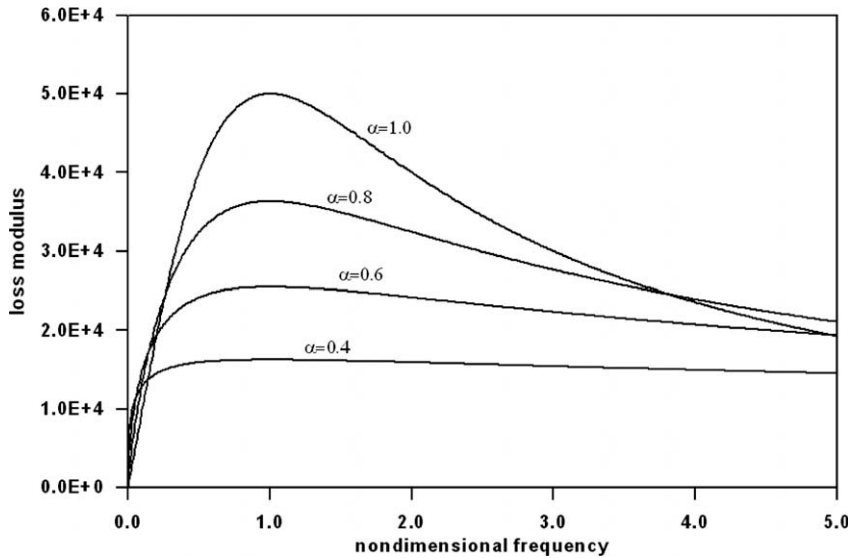


Fig. 3. The loss modulus of the fractional Maxwell model for different values of  $\alpha$  parameter.

Taking into account that (see [34, p. 311])

$$D_t^\alpha q(t) = \lambda^\alpha q_0 \sin[\lambda t + (\alpha\pi/2)], \quad (23)$$

and introducing (22) and (23) into Eq. (2) we can write

$$u(t) = k[1 + (\tau\lambda)^\alpha \cos(\alpha\pi/2)]q_0 \sin \lambda t + k(\tau\lambda)^\alpha q_0 \sin(\alpha\pi/2) \cos \lambda t. \quad (24)$$

Next, using (22) and the identity  $\sin^2(\alpha\pi/2) + \cos^2(\alpha\pi/2) = 1$ , we can rewrite (24) in the form of the following equation

$$\left\{ \frac{u(t) - k[1 + (\tau\lambda)^\alpha \cos(\alpha\pi/2)]q(t)}{k(\tau\lambda)^\alpha q_0 \sin(\alpha\pi/2)} \right\}^2 + \left[ \frac{q(t)}{q_0} \right]^2 = 1, \quad (25)$$

which describes the first version of the hysteresis loop of the fractional Kelvin–Voigt model.

Derivation of the second version of the hysteresis loop started with an assumption that the damper's displacement is described by

$$q(t) = q_0 \sin[\lambda t - (\alpha\pi/2)], \quad (26)$$

which means that

$$D_t^\alpha q(t) = \lambda^\alpha q_0 \sin \lambda t. \quad (27)$$

Introducing relationship (26) into the motion Eq. (2) we can write

$$u(t) - k\tau^\alpha D_t^\alpha q(t) = kq_0[\sin \lambda t \cos(\alpha\pi/2) - \cos \lambda t \sin(\alpha\pi/2)]. \quad (28)$$

Using (27) it is possible to write the second version of the hysteresis loop equation in the following form:

$$\left\{ \frac{u(t) - k\lambda^{-\alpha}[(\tau\lambda)^\alpha + \cos(\alpha\pi/2)]D_t^\alpha q(t)}{kq_0 \sin(\alpha\pi/2)} \right\}^2 + \left[ \frac{D_t^\alpha q(t)}{\lambda^\alpha q_0} \right]^2 = 1. \quad (29)$$

In a case of the classical Kelvin–Voigt model we have:

$$\left[ \frac{u(t) - kq(t)}{\lambda c q_0} \right]^2 + \left[ \frac{q(t)}{q_0} \right]^2 = 1, \quad \left[ \frac{u(t) - c\dot{q}(t)}{kq_0} \right]^2 + \left[ \frac{\dot{q}(t)}{\lambda q_0} \right]^2 = 1, \quad (30)$$

instead of (25) and (29).

Let us now proceed to developing the equation describing the hysteresis loop of the fractional Maxwell model. The excitation is described by

$$u(t) = u_0 \sin \lambda t, \tag{31}$$

what means that

$$D_t^\alpha u(t) = \lambda^\alpha u_0 \sin[\lambda t + (\alpha\pi/2)]. \tag{32}$$

Introducing (32) into the motion Eq. (4) we obtain the following relationship

$$u(t) - k\tau^\alpha D_t^\alpha q(t) = -(\tau\lambda)^\alpha u_0 [\sin \lambda t \cos(\alpha\pi/2) + \cos \lambda t \sin(\alpha\pi/2)], \tag{33}$$

which could be rewritten as

$$\left\{ \frac{k\tau^\alpha D_t^\alpha q(t) - [1 + (\tau\lambda)^\alpha \cos(\alpha\pi/2)]u(t)}{(\tau\lambda)^\alpha u_0 \sin(\alpha\pi/2)} \right\}^2 + \left[ \frac{u(t)}{u_0} \right]^2 = 1. \tag{34}$$

This is the first version of the hysteresis loop equation of the fractional Maxwell model.

To obtain the second version of the hysteresis loop equation the motion Eq. (4) must be fractionally integrated. This operation is formally defined in [34] and here it will be denoted using the symbol  $D_t^{-\alpha} u(t)$  if the function  $u(t)$  is integrated. Moreover, it can be demonstrated that  $D_t^{-\alpha} (D_t^\alpha u(t)) = u(t)$ .

After the fractional integration of Eq. (4) we obtain

$$D_t^{-\alpha} u(t) + \tau^\alpha u(t) = k\tau^\alpha q(t). \tag{35}$$

Now, if  $u(t)$  is given by (31) then

$$D_t^{-\alpha} (u_0 \sin \lambda t) = u_0 \lambda^{-\alpha} \sin[\lambda t - (\alpha\pi/2)]. \tag{36}$$

Introducing (31) into (4) we can write Eq. (35) in the form:

$$k(\tau\lambda)^\alpha q(t) - (\tau\lambda)^\alpha u(t) = u_0 [\sin \lambda t \cos(\alpha\pi/2) - \cos \lambda t \sin(\alpha\pi/2)]. \tag{37}$$

Next, with the help of relationships (31) and  $\sin^2(\alpha\pi/2) + \cos^2(\alpha\pi/2) = 1$  we can transform the above equation to

$$\left\{ \frac{k(\tau\lambda)^\alpha q(t) - [(\tau\lambda)^\alpha + \cos(\alpha\pi/2)]u(t)}{u_0 \sin(\alpha\pi/2)} \right\}^2 + \left[ \frac{u(t)}{u_0} \right]^2 = 1, \tag{38}$$

which is the second version of the hysteresis loop equation searched for.

It is obvious that, for the classical Maxwell model ( $\alpha = 1$ ) we obtain:

$$\left[ \frac{c\dot{q}(t) - u(t)}{\tau\lambda u_0} \right]^2 + \left[ \frac{u(t)}{u_0} \right]^2 = 1, \quad (\tau\lambda)^2 \left[ \frac{kq(t) - u(t)}{u_0} \right]^2 + \left[ \frac{u(t)}{u_0} \right]^2 = 1, \tag{39}$$

instead of (34) and (38), respectively.

The hysteresis loops of the fractional Kelvin–Voigt model and the fractional Maxwell model are shown in Figs. 4 and 5, respectively, for different values of  $\alpha$  and for  $k = 1,00,000.0 \text{ N/m}$ ,  $c = 1,00,000.0 \text{ Ns/m}$ ,  $\lambda = 10.0 \text{ rad/s}$ . It is evident that for both models the damper's damping abilities decrease as the values of  $\alpha$  decrease.

### 3. General remarks concerning identification methods

The problem of determination of the parameters of the fractional derivative rheological models is, more or less extensively, discussed in papers [10,13,17,20,21,37–40]. In two papers [10,13], Pritz describes the method of parameters identification of two fractional derivative rheological models with four and five parameters, respectively. The method utilizes some asymptotic properties of the storage and loss modulus functions, experimen-

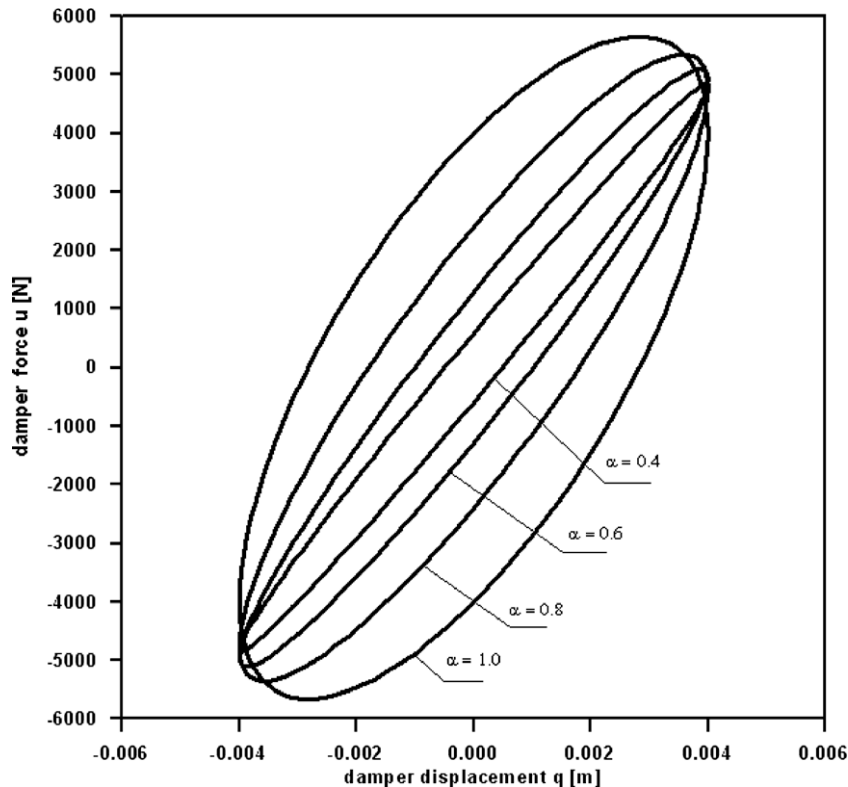


Fig. 4. Hysteresis loops of the fractional Kelvin–Voigt model for different values of  $\alpha$ .

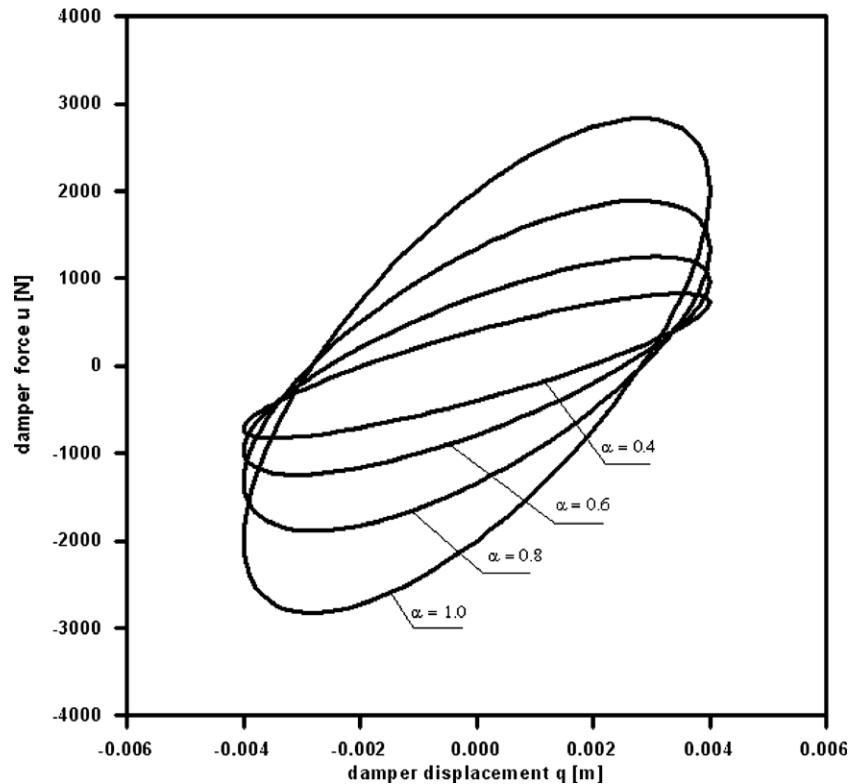


Fig. 5. Hysteresis loops of the fractional Maxwell model for different values of  $\alpha$ .

tally obtained over a certain range of excitation frequencies. However, no systematic procedure of identification is presented. Similar methods are developed in [20,38] where more detailed description of identification procedure is also presented. The above mentioned methods require experimental data from a large range of excitation frequencies. Very recently, in paper [39], the identification procedure of parameters of fractional derivative model of viscoelastic materials is also presented. The method uses an optimization procedure together with the experimentally and numerically obtained frequency response functions to determine the parameters of the considered model VE materials. The differences between the measured and calculated frequency response functions are minimized in order to estimate the true values of the searched parameters. Moreover, the least squares method, in which the error between the model and the experimental complex modulus  $K^*(\lambda)$ , ( $K^*(\lambda) = K'(\lambda) + iK''(\lambda)$ ) is minimized in order to obtain the parameters of the fractional model of viscoelastic materials is suggested in [21,37,40]. Unfortunately, details of the used least squares method are presented in [40] only.

There are many papers containing a description of the method of identification of parameters of the classic rheological models of VE materials and VE dampers. In paper [4] Park used the Prony series together with the least squares method to determine parameters of the generalized Maxwell model of the VE solid and the VE liquid damper. The normalized error between the experimentally obtained and the calculated complex modulus is minimized. The optimization problem is linear because the number of Prony series and the relaxation times are fixed. The last square method is also used in [6] to determine the parameters of two mechanical models of VE dampers. The models are the Kelvin chain and the Maxwell ladder. Some information concerning identification of the parameters of the so-called GHM model and the ADF model used for modeling viscoelastic materials are presented in [41]. The advanced numerical methods for parameter identification of VE materials are presented in [8,9,42] where the least squares method together

with the regularization technique is used to solve the considered identification problem.

In this paper, the parameters of the fractional Kelvin model and the fractional Maxwell model are determined using results of dynamic tests. The proposed identification methods differ substantially in comparison with the previously mentioned ones. First of all, instead of using the experimentally obtained complex modulus the suggested methods utilize the measured steady state responses of damper. The previous methods, presented in [10,13,20,38], require experimental data from a large range of excitation frequency while the suggested methods could be also used when data are available only from a narrow range of excitation frequency. Moreover, the error functional minimized in the least squares method and adopted in our identification methods is different from one used in previous papers. The results of calculation show that the proposed methods are not sensitive to measurements noises and, therefore, it is not necessary to use regularization techniques. Additionally, a detailed description of the proposed identification method and the identification procedure are presented.

Three kinds of identification methods are suggested in this paper to determine three parameters of the fractional Kelvin–Voigt model and the fractional Maxwell model. Each identification procedure consists of two main steps. In the first step, for the given frequencies of excitation, experimentally obtained data are approximated by simple harmonic functions while model parameters are determined in the second stage of the identification procedure.

#### 4. Identification of model parameters for fractional Kelvin–Voigt model

##### 4.1. Identification procedures based on hysteresis loop (first method)

First of all, the first kind method based on the hysteresis loop and applied to the fractional Kelvin–Voigt model will be described.

Eq. (25) seems to be more useful in comparison with (29). If, for the given frequency of excitation and  $t = t_1$ , we have  $q(t_1) = q_0 > 0$  and  $u(t_1) = u_1 > 0$  then from Eq. (25) it follows

$$k[1 + (\tau\lambda)^\alpha \cos(\alpha\pi/2)] = k + c\lambda^\alpha \cos(\alpha\pi/2) = u_1/q_0. \quad (40)$$

Moreover, for  $t = t_2$  when  $q(t_2) = 0$  and  $u(t_2) = u_2 > 0$  from (25) we obtain

$$k(\tau\lambda)^\alpha \sin(\alpha\pi/2) = c\lambda^\alpha \sin(\alpha\pi/2) = u_2/q_0. \quad (41)$$

For a given frequency  $\lambda$ , relationships (40) and (41) constitute a set of two nonlinear equations with three unknowns:  $k, c, \alpha$  or  $k, \tau, \alpha$ . The quantities  $u_1, u_2$  and  $q_0$  have clear physical meanings and their values can easily be obtained from the experimental data. Alternatively, these quantities could be calculated from trigonometric functions (A1) and (A6) used for the approximation of experimental data. Details are given in Appendix A. For a given  $\alpha$ , the above set of equations are linear with respect to  $k$  and  $c$ .

During experiments the damper is several times harmonically excited and in each case the excitation frequency, denoted here as  $\lambda_i$ , ( $i = 1, 2, \dots, n$ ), is different. The steady state response of the damper is measured, which means that the experimental damper displacements  $q_{ei}(t)$  and the experimental damper forces  $u_{ei}(t)$  and functions  $\tilde{q}_i(t)$   $\tilde{u}_i(t)$  which approximate the experimental data are known for each excitation frequency  $\lambda_i$ . Moreover, the above mentioned quantities, such as  $u_1, u_2$  and  $q_0$  can easily be determined for each excitation frequency. These quantities obtained from experimental data are denoted as  $u_{1i}, u_{2i}$  and  $q_{0i}$ .

Now it is assumed that resulting quantities  $u_{1i}, u_{2i}$  and  $q_{0i}$  approximately fulfill relationships (40) and (41). For each excitation frequency we can write

$$r_i = k + c\lambda_i^\alpha \cos(\alpha\pi/2) - u_{1i}/q_{0i} \approx 0, \quad (42)$$

$$s_i = c\lambda_i^\alpha \sin(\alpha\pi/2) - u_{2i}/q_{0i} \approx 0, \quad (43)$$

where  $i = 1, 2, \dots, n$ . Symbols  $r_i$  and  $s_i$  denote residuals obtained after introducing  $u_{1i}, u_{2i}$  and  $q_{0i}$  into (42) and (43).

The above equations constitute a set of overdetermined nonlinear equations with respect to  $k, c$  and  $\alpha$ . A pseudo-solution to the above system of equation is chosen in such a way that it minimizes the following functional

$$\tilde{J}_{KV}(k, c, \alpha) = \sum_{i=1}^n (r_i^2 + s_i^2). \quad (44)$$

If we assume that the parameter  $\alpha$  is known, then stationary conditions:

$$\frac{\partial \tilde{J}_{KV}(k, c, \alpha)}{\partial k} = 0, \quad \frac{\partial \tilde{J}_{KV}(k, c, \alpha)}{\partial c} = 0. \quad (45)$$

give us the following set of equations, which are linear with respect to  $k$  and  $c$

$$kn + c \sum_{i=1}^n \lambda_i^\alpha \cos(\alpha\pi/2) = \sum_{i=1}^n \frac{u_{1i}}{q_{0i}},$$

$$k \sum_{i=1}^n \lambda_i^\alpha \cos(\alpha\pi/2) + c \sum_{i=1}^n \lambda_i^{2\alpha} = \sum_{i=1}^n \lambda_i^\alpha \left[ \frac{u_{1i}}{q_{0i}} \cos(\alpha\pi/2) + \frac{u_{2i}}{q_{0i}} \sin(\alpha\pi/2) \right]. \quad (46)$$

The right value of  $\alpha$  is obtained using the systematic searching method. The set of values of  $\alpha$ , denoted as  $\alpha_j$  ( $j = 1, 2, \dots, m$ ), where  $\alpha_j = \alpha_{j-1} + \Delta\alpha$  is chosen from a given range of  $\alpha$ . For each  $\alpha_j$  the corresponding values of  $k$  and  $c$  (denoted as  $k_j$  and  $c_j$ ) are determined from (46) and the value of functional (44) is calculated. These values of  $\alpha_j, k_j$  and  $c_j$  for which the functional (44) has a minimum value are the searched parameters of the fractional Kelvin–Voigt damper model.

#### 4.2. Identification procedures based on time series data (second and third method)

The identification procedure based on time series data is also developed. The second-kind method will be described first. The experimentally measured damper displacement is approximated using the harmonic function (A1). The parameters  $\tilde{q}_c$  and  $\tilde{q}_s$  are obtained from the set of Eq. (A3).

Moreover, it is assumed that the experimentally obtained steady state solution represented by the harmonic function (A1) approximately fulfills the steady state Eq. (18) of the fractional Kelvin model where  $\tilde{q}_c$  and  $\tilde{q}_s$  are introduced in a place of  $q_c$  and  $q_s$ , respectively.

Now, for a given excitation frequency  $\lambda$ , the quantities  $\varphi_1$  and  $\varphi_2$ , appearing in (18), are determined as described below. The right values of  $\varphi_1$  and  $\varphi_2$  are the ones which minimize the functional

$$J_{KV}(\varphi_1, \varphi_2) = \frac{1}{t_2 - t_1} \int_{t_1}^{t_2} [u_e(t) - u(t)]^2 dt. \quad (47)$$

considered here as the functional of  $\varphi_1$  and  $\varphi_2$ . Stationary conditions of the above-mentioned functional give us the following linear equations with respect to  $\varphi_1$  and  $\varphi_2$

$$a_{11}\varphi_1 + a_{12}\varphi_2 = b_1, \quad a_{21}\varphi_1 + a_{22}\varphi_2 = b_2, \quad (48)$$

where coefficients  $a_{11}, a_{12}, a_{21}, a_{22}, b_1$  and  $b_2$  are given by

$$a_{11} = \tilde{q}_c^2 I_{cc} + 2\tilde{q}_c \tilde{q}_s I_{cs} + \tilde{q}_s^2 I_{ss}, \quad a_{12} = a_{21} = \tilde{q}_c \tilde{q}_s (I_{cc} - I_{ss}) + (\tilde{q}_s^2 - \tilde{q}_c^2) I_{cs}, \quad (49)$$

$$a_{22} = \tilde{q}_c^2 I_{ss} - 2\tilde{q}_c \tilde{q}_s I_{cs} + \tilde{q}_s^2 I_{cc}, \quad b_1 = \tilde{q}_c I_{cu} + \tilde{q}_s I_{su}, \quad b_2 = -\tilde{q}_c I_{su} + \tilde{q}_s I_{cu}, \quad (50)$$

$$I_{cu} = \int_{t_1}^{t_2} u_e(t) \cos \lambda t dt, \quad I_{su} = \int_{t_1}^{t_2} u_e(t) \sin \lambda t dt, \quad (51)$$

$$I_{cq} = \int_{t_1}^{t_2} q_e(t) \cos \lambda t dt, \quad I_{sq} = \int_{t_1}^{t_2} q_e(t) \sin \lambda t dt. \quad (52)$$

The solution to Eq. (48) is

$$\varphi_1 = \frac{b_1 a_{22} - b_2 a_{12}}{a_{11} a_{22} - a_{12} a_{21}}, \quad \varphi_2 = \frac{-b_1 a_{21} + b_2 a_{11}}{a_{11} a_{22} - a_{12} a_{21}}. \quad (53)$$

During experiments, the data are measured for different excitation frequencies  $\lambda_i$ , ( $i = 1, 2, \dots, n$ ) and subsequently the values of  $\varphi_1$  and  $\varphi_2$ , denoted now as  $\varphi_{1i}$  and  $\varphi_{2i}$ , respectively, are calculated from (48) or (53). For each particular excitation frequency  $\lambda_i$  the following equations, very similar to (42) and (43), could be written:

$$r_i = k + c\lambda_i^\alpha \cos(\alpha\pi/2) - \varphi_{1i} = 0, \quad s_i = c\lambda_i^\alpha \sin(\alpha\pi/2) - \varphi_{2i} = 0. \quad (54)$$

The solutions to a set of overdetermined equations (i.e. Eq. (54) written for  $i = 1, 2, \dots, n$ ) are found in a similar way as in the first identification procedure described above. The searched pseudo-solution minimizes the functional (44) with  $r_i$  and  $s_i$  defined by formulae (54). For a given value of  $\alpha$ , the parameters  $k$  and  $c$  fulfill the equations

$$kn + c \sum_{i=1}^n \lambda_i^\alpha \cos(\alpha\pi/2) = \sum_{i=1}^n \varphi_{1i},$$

$$k \sum_{i=1}^n \lambda_i^\alpha \cos(\alpha\pi/2) + c \sum_{i=1}^n \lambda_i^{2\alpha} = \sum_{i=1}^n \lambda_i^\alpha [\varphi_{1i} \cos(\alpha\pi/2) + \varphi_{2i} \sin(\alpha\pi/2)], \quad (55)$$

and the parameter  $\alpha$  is obtained with the help of the systematic searching method described earlier in this paper. One can see that Eq. (55) are very similar to Eq. (46).

Please note, in this procedure only the data concerning the damper displacement  $q_e(t)$  are approximated using the trigonometric function.

The second identification procedure based on in-time data series (called here the third-kind method) will also be formulated for the fractional Kelvin–Voigt model. In this procedure, experimentally measured variations of both the damper force and the damper displacement are approximated using the harmonic functions (A1) and (A6), respectively. Moreover, it is assumed that Eq. (18) are approximately fulfilled when  $\tilde{q}_c, \tilde{q}_s, \tilde{u}_c$  and  $\tilde{u}_s$  are introduced in a place of  $q_c, q_s, u_c$  and  $u_s$ , respectively. Now, from Eq. (18) we obtain

$$\varphi_1 = \frac{\tilde{q}_c \tilde{u}_c + \tilde{q}_s \tilde{u}_s}{\tilde{q}_c^2 + \tilde{q}_s^2}, \quad \varphi_2 = \frac{\tilde{q}_s \tilde{u}_c - \tilde{q}_c \tilde{u}_s}{\tilde{q}_c^2 + \tilde{q}_s^2}. \quad (56)$$

The quantities  $\varphi_1$  and  $\varphi_2$  obtained for a particular frequency of vibration  $\lambda_i$ , will be denoted as  $\varphi_{1i}$  and  $\varphi_{2i}$ , respectively. For a given set of excitation frequencies  $\lambda_i, (i = 1, 2, \dots, n)$ , the overdetermined set of Eq. (54) could be written.

The values of model parameters  $k, c$  and  $\alpha$  are chosen in such a way that the functional (44) will be minimized ( $r_i$  and  $s_i$  are defined by relationships (54)). The procedure described in this subsection could be used without being modified at all. The right value of  $\alpha$  is obtained using the systematic searching method and the values of the associated parameters  $k$  and  $c$  are determined from the set of Eq. (55).

It is easy to notice that both of the methods described above differ only in the way  $\varphi_{1i}$  and  $\varphi_{2i}$  are calculated. The first identification procedure based on in-time series approximate the experimental data concerning the damper displacement with the help of the trigonometric function while the third-kind method used this approximation for both experimental data.

### 5. Identification of model parameters for fractional Maxwell model

#### 5.1. Identification procedures based on hysteresis loop (first method)

A similar method to the one described in Section 4.1 is developed for the fractional Maxwell model. For a given excitation frequency  $\lambda$  and  $t = t_1$ , when  $u(t_1) = u_0 > 0$  and  $q(t_1) = q_1 > 0$ , from Eq. (38) we obtain:

$$k(\tau\lambda)^\alpha q_1 - (\tau\lambda)^\alpha u_0 - u_0 \cos(\alpha\pi/2) = 0, \quad (57)$$

which could also be written in the form:

$$c\lambda^\alpha q_1 - \tilde{\tau}\lambda^\alpha u_0 - u_0 \cos(\alpha\pi/2) = 0. \quad (58)$$

Moreover, at  $t = t_2$  when the state of the damper is described by  $u(t_2) = 0$  and  $q(t_2) = q_2 < 0$ , from the hysteresis loop Eq. (38) it follows:

$$k(\tau\lambda)^\alpha q_2 + u_0 \sin(\alpha\pi/2) = 0, \quad (59)$$

which subsequently could be rewritten in the form:

$$c\lambda^\alpha q_2 + u_0 \sin(\alpha\pi/2) = 0. \quad (60)$$

If we have experimental data for a given set of excitation frequencies  $\lambda_i, (i = 1, 2, \dots, n)$  then the following set of equations (with respect to  $c, \tilde{\tau}$  and  $\alpha$ )

$$\begin{aligned} r_i &= c\lambda_i^\alpha q_{1i} - \tilde{\tau}\lambda_i^\alpha u_{0i} - u_{0i} \cos(\alpha\pi/2) = 0, \\ s_i &= c\lambda_i^\alpha q_{2i} + u_{0i} \sin(\alpha\pi/2) = 0, \end{aligned} \quad (61)$$

could be written.

As in the previous model, a pseudo-solution to the above set of equations is chosen as one which minimized the functional:

$$\tilde{J}_M(c, \tilde{\tau}, \alpha) = \sum_{i=1}^n (r_i^2 + s_i^2). \quad (62)$$

If we assume that the parameter  $\alpha$  is known, the stationary conditions of (62) give us the following system of equations:

$$\begin{aligned} c \sum_{i=1}^n \lambda_i^{2\alpha} (q_{1i}^2 + q_{2i}^2) - \tilde{\tau} \sum_{i=1}^n \lambda_i^{2\alpha} u_{0i} q_{1i} \\ = \sum_{i=1}^n \lambda_i^{2\alpha} u_{0i} [q_{1i} \cos(\alpha\pi/2) - q_{2i} \sin(\alpha\pi/2)], \\ -c \sum_{i=1}^n \lambda_i^{2\alpha} u_{0i} q_{1i} + \tilde{\tau} \sum_{i=1}^n \lambda_i^{2\alpha} u_{0i}^2 = -\sum_{i=1}^n \lambda_i^{2\alpha} u_{0i}^2 \cos(\alpha\pi/2). \end{aligned} \quad (63)$$

For particular values of  $\alpha$ , the values of damper parameters resulting from (61) could be negative. These values do not have physical meaning and must be rejected.

As described in Section 4.1, the right value of  $\alpha$  is obtained using the method of systematic searching. The values of  $\alpha, \tilde{\tau}$  and  $c$  for which the functional (62) has a minimum value are the searched parameters of the fractional Maxwell model.

#### 5.2. Identification procedures based on time series data (second and third method)

In the second-kind method, for the given frequency of excitation the experimentally measured damper force  $u_e(t)$  is approximated using function (A6) where  $\tilde{u}_c$  and  $\tilde{u}_s$  are determined from Eq. (A8). The steady state solution to the equation of motion (4) is given by (16) and (17) and the coefficients  $q_c, q_s, u_c$  and  $u_s$  are interrelated as it is given by relation (20).

Next,  $\tilde{u}_c$  and  $\tilde{u}_s$ , obtained from the experimental data and for the given frequency of excitation  $\lambda$ , are introduced in relationships (20) in the place of  $u_c$  and  $u_s$  and the functional

$$J_M(\phi_1, \phi_2) = \frac{1}{t_2 - t_1} \int_{t_1}^{t_2} [q_e(t) - q(t)]^2 dt, \quad (64)$$

is minimized with respect to  $\phi_1$  and  $\phi_2$ . The stationary conditions of this functional give us the following set of equations

$$a_{11}\phi_1 + a_{12}\phi_2 = b_1, \quad a_{21}\phi_1 + a_{22}\phi_2 = b_2, \quad (65)$$

where

$$a_{11} = I_{cc}\tilde{u}_c^2 + 2\tilde{u}_c\tilde{u}_s I_{sc} + \tilde{u}_s^2 I_{ss}, \quad a_{22} = \tilde{u}_c^2 I_{ss} - 2\tilde{u}_c\tilde{u}_s I_{sc} + \tilde{u}_s^2 I_{cc}, \quad (66)$$

$$a_{12} = a_{21} = (\tilde{u}_c^2 - \tilde{u}_s^2) I_{sc} + \tilde{u}_c\tilde{u}_s (I_{ss} - I_{cc}), \quad (67)$$

$$b_1 = \tilde{u}_c I_{cq} + \tilde{u}_s I_{sq}, \quad b_2 = \tilde{u}_c I_{sq} - \tilde{u}_s I_{cq}. \quad (68)$$

The values  $I_{ss}, I_{sc}, I_{cc}$  are defined by the relationships (A4) and  $I_{sq}, I_{cq}$  by (A5).

The values of  $\phi_1$  and  $\phi_2$ , determined from the set of Eq. (65), is given by

$$\phi_1 = \frac{b_1 a_{11} - b_2 a_{12}}{a_{11} a_{22} - a_{12} a_{21}}, \quad \phi_2 = \frac{-b_1 a_{21} + b_2 a_{11}}{a_{11} a_{22} - a_{12} a_{21}}. \quad (69)$$

The model parameters  $c, k$  and  $\alpha$  will be determined using the least-square method. As previously, the error functional (62), where

$$r_i = \frac{1}{k} + \frac{1}{c} \lambda_i^{-\alpha} \cos \frac{\alpha\pi}{2} - \phi_{1i}, \quad s_i = \frac{1}{c} \lambda_i^{-\alpha} \sin \frac{\alpha\pi}{2} - \phi_{2i}, \quad (70)$$

is minimized with respect to model parameters. The residuals  $r_i$  and  $s_i$  are obtained from relationships (21) after introducing  $\lambda_i$  instead of  $\lambda$  and taking into account that (21) could only approximately be satisfied. As previously, the index  $i$  of such quantities as  $\phi_{1i}$  emphasizes their dependence on the  $i$ -th frequency of excitation used in the experiments.

The parameter  $\alpha$  is determined with the help of the searching method described earlier, while the values of  $c$  and  $k$  are obtained from the following set of equations:

$$\begin{aligned} n\bar{k} + \bar{c} \sum_{i=1}^n \lambda_i^{-\alpha} \cos(\alpha\pi/2) &= \sum_{i=1}^n \phi_{1i}, \\ \bar{k} \sum_{i=1}^n \lambda_i^{-\alpha} \cos(\alpha\pi/2) + \bar{c} \sum_{i=1}^n \lambda_i^{-2\alpha} &= \sum_{i=1}^n \lambda_i^{-\alpha} [\phi_{1i} \cos(\alpha\pi/2) + \phi_{2i} \sin(\alpha\pi/2)], \end{aligned} \quad (71)$$

where  $\bar{k} = 1/k$  and  $\bar{c} = 1/c$ .

The third-kind method, applied to the fractional Maxwell model, utilizes the functions  $\tilde{q}(t)$  and  $\tilde{u}(t)$ , described, for  $\lambda = \lambda_i$ , by relationships (A1) and (A6). The parameters  $\tilde{u}_{ci}, \tilde{u}_{si}, \tilde{q}_{ci}$  and  $q_{si}$  introduced now in a place of  $\tilde{u}_c, \tilde{u}_s, \tilde{q}_c$  and  $q_s$  approximately fulfill the following equations

$$\tilde{q}_{ci} = \phi_{1i} \tilde{u}_{ci} - \phi_{2i} \tilde{u}_{si}, \quad \tilde{q}_{si} = \phi_{2i} \tilde{u}_{ci} + \phi_{1i} \tilde{u}_{si}, \quad (72)$$

resulting from Eq. (20). From the equations above we have

$$\phi_{1i} = \frac{\tilde{q}_{ci} \tilde{u}_{ci} + \tilde{q}_{si} \tilde{u}_{si}}{\tilde{u}_{ci}^2 + \tilde{u}_{si}^2}, \quad \phi_{2i} = \frac{\tilde{q}_{si} \tilde{u}_{ci} - \tilde{q}_{ci} \tilde{u}_{si}}{\tilde{u}_{ci}^2 + \tilde{u}_{si}^2}. \quad (73)$$

Model parameters are determined with the help of the procedure described above, where the error functional (62) and the identical searching procedure together with relationships (70) and (71) are used.

For the fractional Maxwell model both of the methods described in this subsection differ only in the way  $\phi_{1i}$  and  $\phi_{2i}$  are calculated.

The reciprocal comparison of all proposed identification methods makes it possible to formulate the following remarks:

- (a) as proved in Section 6, none of the proposed methods is sensitive to measurements noises,
- (b) for both rheological models the second-kind method and the third-kind method differ only in the way in which  $\phi_{1i}$  and  $\phi_{2i}$  or  $\varphi_{1i}$  and  $\varphi_{2i}$  are calculated,
- (c) the second-kind method analytically approximates experimental data obtained for the damper displacement (the Kelvin–Voigt model) or only for the damper force (in the case of the Maxwell model) while the third-kind method analytically approximates the experimental data for both the damper displacement and the damper force,
- (d) similar calculation efforts are needed when each of the presented methods is used to identify the dampers parameters,
- (e) any existing differences between the discussed methods have no significant influence on the effectiveness of the methods and on the results of identification.

## 6. Algorithms of identification methods and results of typical calculation

### 6.1. Algorithms of identification methods

All of the identification procedures have some similarities which were mentioned, to some extent, in previous Subsections. Generally speaking, all algorithms consist of three steps. Approximation of the experimental data using the trigonometric functions is made in the first step. In the second step, some quantities, for example,  $\varphi_{1i}, \varphi_{2i}, \phi_{1i}$  and  $\phi_{2i}$  are calculated for all frequencies of excitation. Finally, the model parameters are determined in the third step. For the readers' convenience, the flowcharts of all of the algorithms are presented in Figs. 6–8.

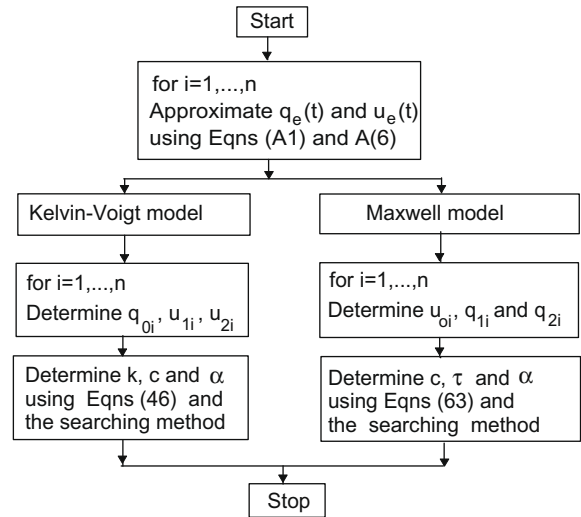


Fig. 6. Flowchart of the procedure of the first-kind identification method.

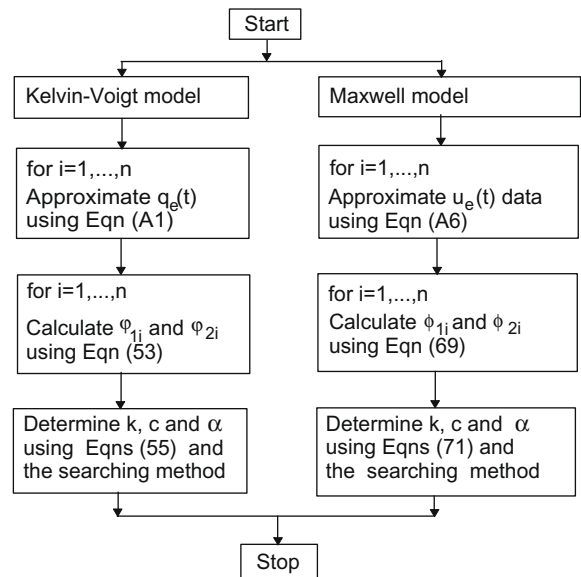


Fig. 7. Flowchart of the procedure of the second-kind identification method.

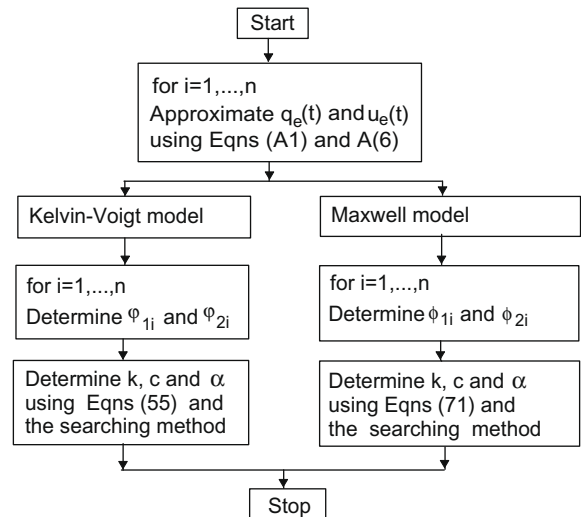


Fig. 8. Flowchart of the procedure of the third-kind identification method.

6.2. Results of typical calculation – the fractional Kelvin–Voigt model

The identification procedure described above is applied to artificial data. The artificial experimental steady state solutions are generated on the basis of the solution to the motion Eq. (2). These solutions are given by functions (16) and (17). If, for example,  $q_c = 0$ , then

$$\begin{aligned} q(t) &= q_s \sin \lambda t, \quad u_1 = q_s k [1 + (\tau \lambda)^\alpha \cos(\alpha \pi / 2)], \\ u_2 &= q_s k (\tau \lambda)^\alpha \sin(\alpha \pi / 2). \end{aligned} \tag{74}$$

The artificial data obtained from relationships (74) are modified by applying small, randomly inserted perturbations. The noises of 1% intensity of the damper force or the damper displacement are applied.

The following data are used to generate artificial experimental data:  $q_s = 0.001$  m,  $q_c = 0$ ,  $k = 2,90,000.0$  N/m,  $c = 68,000.0$  Ns/m,  $\alpha = 0.6$ ,  $n = 9$ . The values of excitation frequencies  $\lambda_i$  chosen in this example and the values of  $u_{1i}$ ,  $u_{2i}$  and  $q_{0i}$  determined from the artificial data are given in Table 1.

After application of the identification procedure based on the hysteresis loop the following results are obtained:  $\alpha = 0.601$ ,  $k = 2,89,936.0$  N/m,  $c = 67,646.8$  Ns/m, which is in good agreement with exact values. Results of calculation performed for different noise levels are presented in Fig. 9. It is easy to notice that the rel-

ative errors of values of  $\alpha$ ,  $k$  and  $c$  parameters are of the order of noises.

The third-kind method is also applied to artificial experimental data described above. The following results are obtained:  $\alpha = 0.609$ ,  $k = 2,92,115.0$  N/m,  $c = 64,984.0$  Ns/m when 3% noises are randomly introduced to artificial data. Relative errors of damper parameter values performed for different noise levels are shown in Fig. 10.

Very good results are obtained using the second-kind method. Following the method presented in [36], random noises is added to the artificial data  $u(t)$  and  $q(t)$  using the formulae:

$$\begin{aligned} u_e(t) &= u(t) + \varepsilon x(t) \sqrt{\text{var}(u(t))}, \\ q_e(t) &= q(t) + \varepsilon z(t) \sqrt{\text{var}(q(t))}, \end{aligned} \tag{75}$$

where  $\varepsilon$  is the noise level,  $x(t)$  and  $z(t)$  are the standard distribution vectors with zero mean and unit deviation,  $\text{var}(u(t))$  and  $\text{var}(q(t))$  are the variation of  $u(t)$  and  $q(t)$ , respectively. Results of calculation performed for different noise levels are presented in Fig. 11. In the considered case, the influence of noises on damper parameters is very small.

The discussed fractional Kelvin–Voigt model was also used to determine the parameters of the small size VE damper. The damper consists of three steel plates and two layers made from viscoelastic material VHB 4959 manufactured by 3M. The thickness of each viscoelastic layer is 3 mm. A harmonically varying excitation with dif-

**Table 1**  
Artificially generated experimental data.

Frequency (Hz)	Fractional Kelvin–Voigt model			Fractional Maxwell model		
	$q_0$ (m)	$u_1$ (N)	$u_2$ (N)	$u_0$ (N)	$q_1$ (m)	$q_2$ (m)
0.5	0.991010e–3	366.564	108.520	297.306	0.232195e–2	–0.177817e–2
1.0	0.991010e–3	414.464	165.182	302.356	0.191155e–2	–0.119442e–2
2.0	1.004310e–3	471.856	250.977	300.441	0.160286e–2	–0.787455e–3
4.0	1.005330e–3	564.810	382.750	299.111	0.140054e–2	–0.517613e–3
6.0	1.000410e–3	637.696	489.893	298.085	0.131743e–2	–0.401366e–3
8.0	0.990801e–3	702.286	580.127	297.083	0.127103e–2	–0.338493e–3
10.0	0.997754e–3	761.647	653.921	300.699	0.125184e–2	–0.295670e–3
12.5	1.007520e–3	834.779	753.747	301.900	0.121994e–2	–0.261395e–3
15.0	0.991348e–3	902.471	836.230	301.531	0.121300e–2	–0.234501e–3

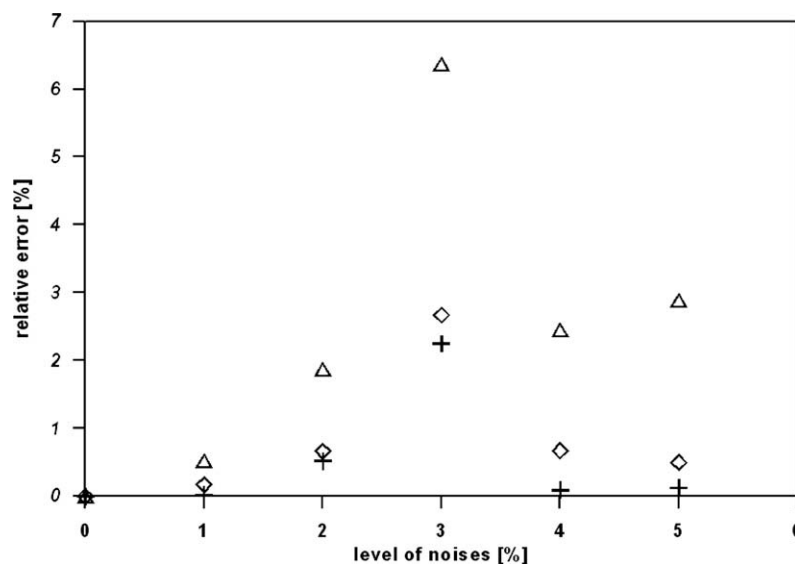


**Fig. 9.** Relative errors of the  $\alpha$  parameter (small rhombs), the  $k$  parameter (small cross marks) and the  $c$  parameter (small triangles) versus the level of noises (the first-kind identification method applied to the Kelvin–Voigt fractional model).

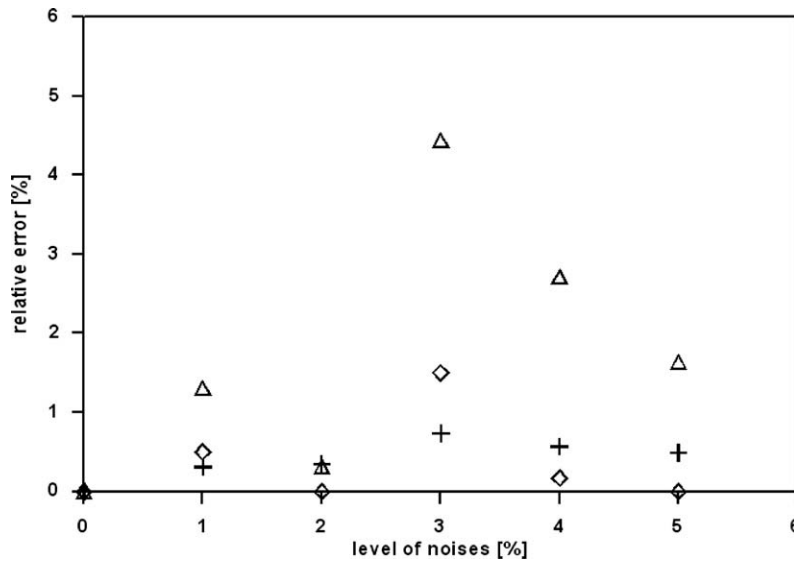


**Fig. 10.** Relative errors of the  $\alpha$  parameter (small rhombs), the  $k$  parameter (small cross marks) and the  $c$  parameter (small triangles) versus the level of noises (the third-kind identification method applied to the Kelvin–Voigt fractional model).

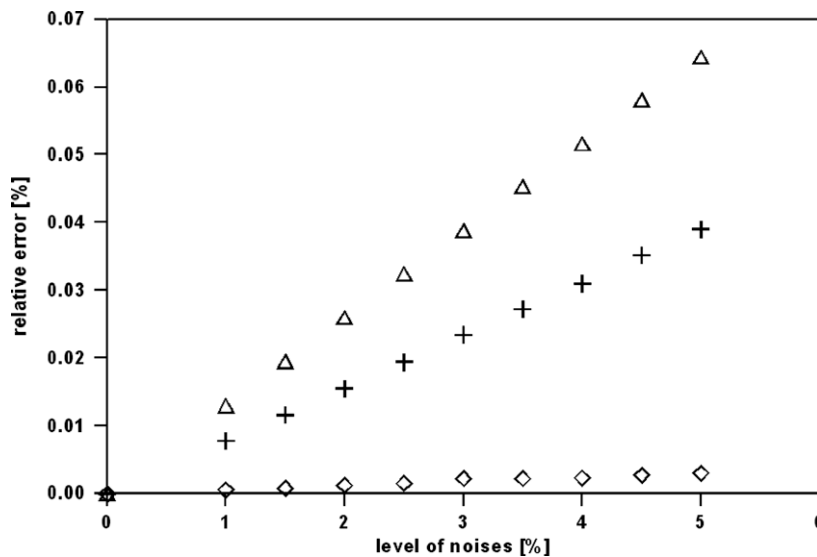


**Fig. 11.** Relative errors of the  $\alpha$  parameter (small rhombs), the  $k$  parameter (small cross marks) and the  $c$  parameter (small triangles) versus the level of noises (the second-kind identification method applied to the Kelvin–Voigt fractional model).

ferent excitation frequencies taken from the range 0.5–15.0 Hz is used during the experiments.

The Kelvin–Voigt model is adopted to describe the VE damper's behaviour. At the beginning, the classical Kelvin–Voigt model, i.e. the fractional model with  $\alpha = 1$ , was used to determine the dampers parameters. In this case, the values of  $k$  and  $c$  parameters can be determined independently for each frequency of excitation from Eqs. (54). The results of calculation based on a times series are presented in Table 2 where values of the parameters  $k$  and  $c$  in dependence on the values of excitation frequency are given. As expected, the model parameters strongly depend on excitation frequency. A comparison of the experimentally obtained hysteresis curve with ones resulting from the identification procedure is made in Fig. 12 where the comparison is given for  $\lambda = 1.0$  Hz. The small cross marks show the experimental data while the solid line presents identification results. The very good agreement between the both curves is obvious.

**Table 2**

Stiffness and damping factors of small damper.

Frequency (rad/s)	$k$ (N/m)	$c$ (Ns/m)
3.14	73303.1	14676.5
6.28	86615.5	9659.6
12.56	98416.0	5927.0
25.12	106055.0	3362.0
37.68	106111.0	2295.0
50.24	105254.0	1702.0
62.80	101254.0	1373.0
78.50	98644.0	1085.0
94.20	86823.0	851.0

The results obtained using the fractional Kelvin–Voigt model and the third-kind method will be briefly described. The following values of model parameters:  $\alpha = 0.3755$ ,  $k = 2603.1$  N/m i  $c =$

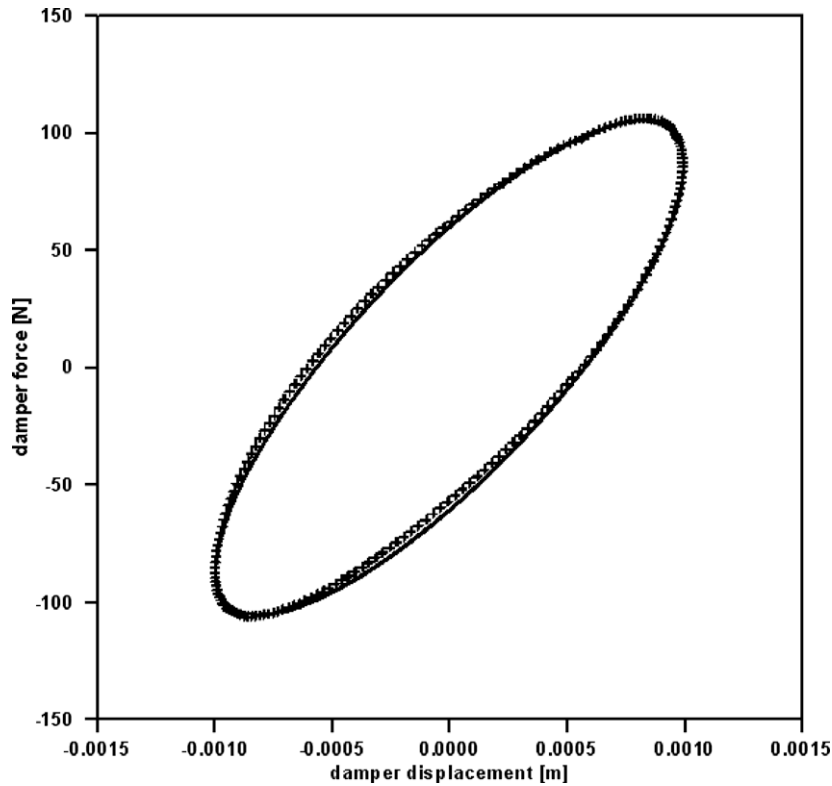


Fig. 12. A comparison of the experimentally obtained hysteresis curve (small cross marks) and the hysteresis curve resulting from the identification procedure (solid line).

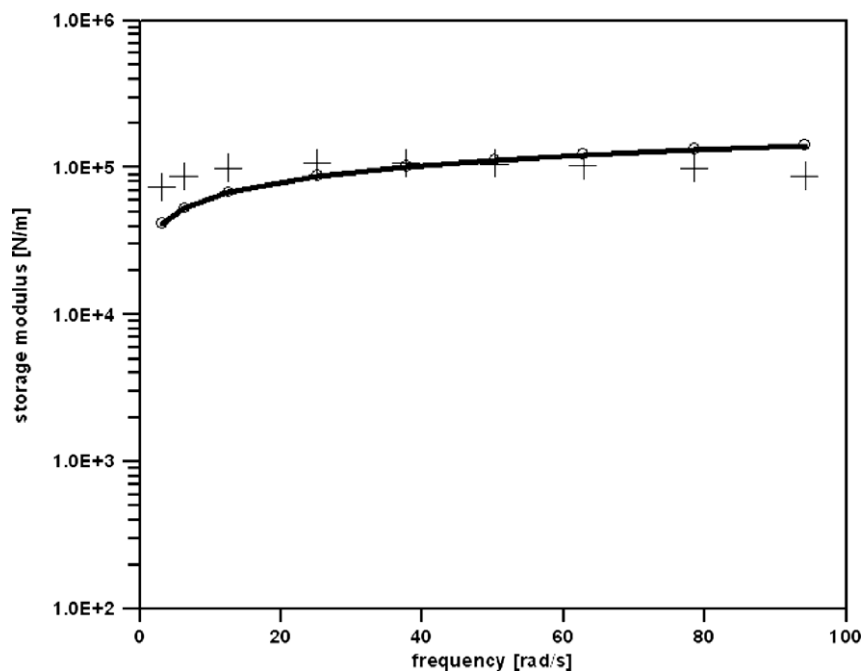


Fig. 13. Storage modulus – comparison of experimental data (small cross marks) with results obtained from the identification procedure (solid line) – the fractional Kelvin–Voigt model.

30,333.9 Ns/m are obtained after application of the identification procedure. A comparison of the storage modulus resulting from the identification procedure (the solid line) with the storage modulus obtained experimentally (the small cross marks) is presented

in Fig. 13. A similar comparison for the loss modulus is shown in Fig. 14. The presented results indicate that the three parameter fractional Kelvin–Voigt model could reasonably well describe the behaviour of solid VE dampers.

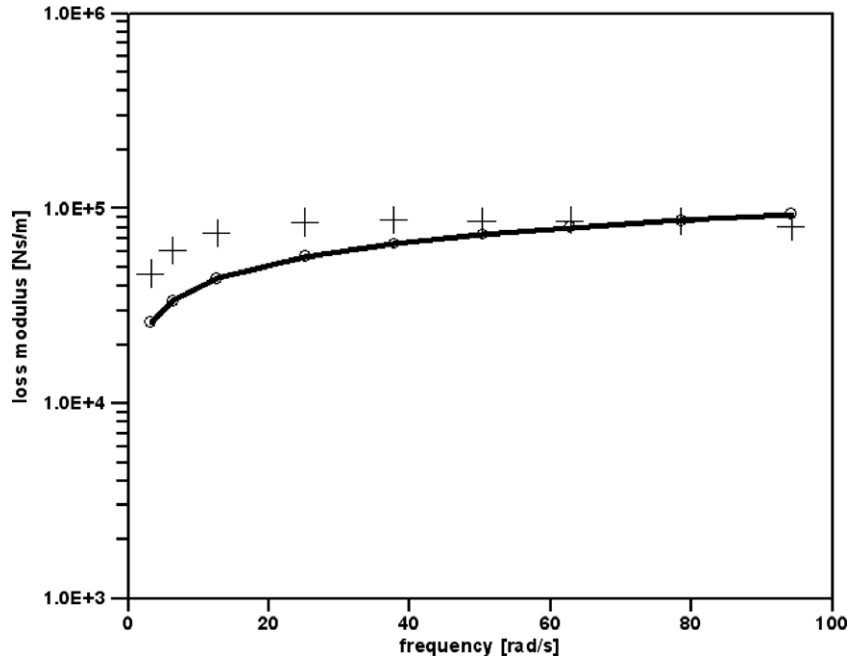


Fig. 14. Loss modulus – comparison of experimental data (small cross marks) with results obtained from the identification procedure (solid line) – the fractional Kelvin–Voigt model.

6.3. Results of typical calculation – the fractional Maxwell model

As previously, the identification procedure described above is applied to artificial data. The artificial experimental steady state solutions are generated on the basis of the solution to Eq. (4). If, for example,  $u_c = 0$  and  $u_0 = u_s$  then

$$q_2 = q_c = -\frac{u_0}{k(\tau\lambda)^\alpha} \sin \frac{\alpha\pi}{2},$$

$$q_1 = q_s = \frac{u_0}{k(\tau\lambda)^\alpha} \left[ (\tau\lambda)^\alpha + \cos \frac{\alpha\pi}{2} \right]. \tag{76}$$

The artificial data are modified by applying small, randomly inserted perturbations.

The following data are used to generate artificial data:  $u_c = 0$ ,  $u_s = u_0 = 300.0$  N,  $k = 2,90,000.0$  N/m,  $c = 68,000.0$  Ns/m,  $\alpha = 0.6$ ,  $n = 9$ . The values of excitation frequencies chosen in this example and values of  $u_{0i}$ ,  $q_{1i}$  and  $q_{2i}$  are given in Table 1.

After application of the identification procedure of first-kind the following results are obtained:  $\alpha = 0.601$ ,  $k = 2,90,469.0$  N/m,  $c = 67,786.2$  Ns/m which is in good agreement with exact values. The results of calculation performed for different noise levels (taken in the range of 0–5 %) are presented in Fig. 15. It is easy to no-

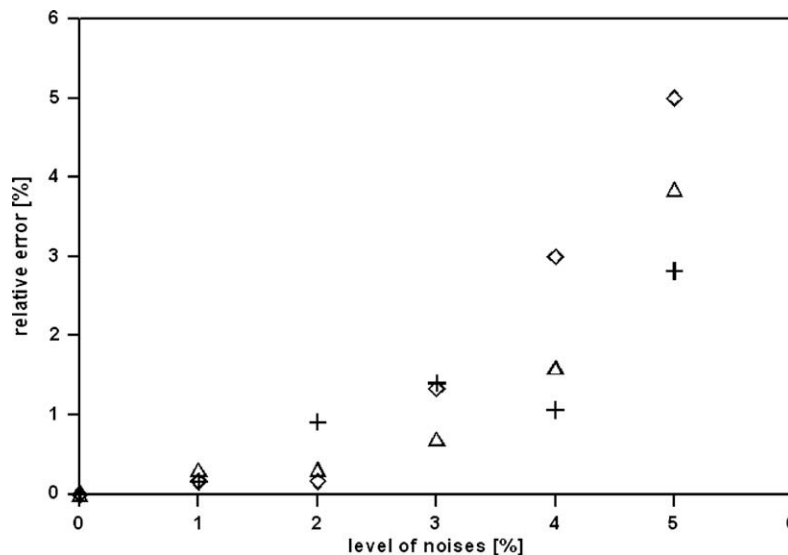


Fig. 15. Relative errors of the  $\alpha$  parameter (small rhombs), the  $k$  parameter (small cross marks) and the  $c$  parameter (small triangles) versus the level of noises (the first-kind identification method applied to the Maxwell fractional model).

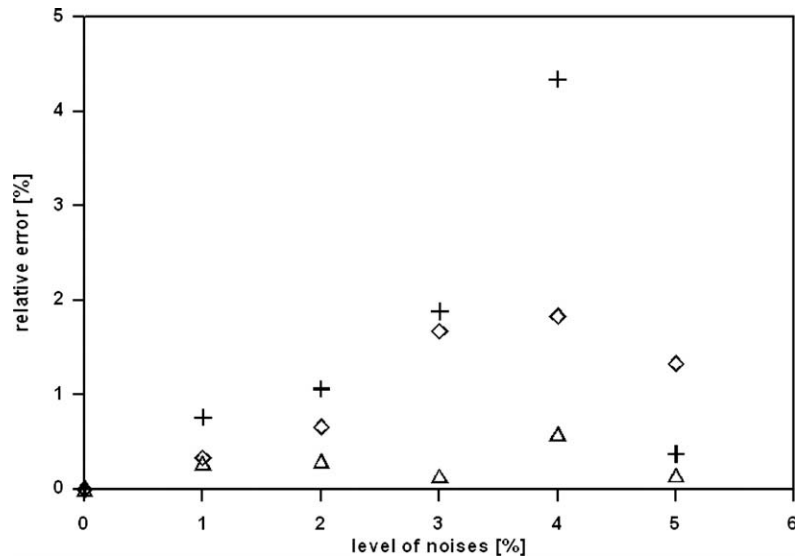


Fig. 16. Relative errors of the  $\alpha$  parameter (small rhombs), the  $k$  parameter (small cross marks) and the  $c$  parameter (small triangles) versus the level of noises (the third-kind identification method applied to the Maxwell fractional model).

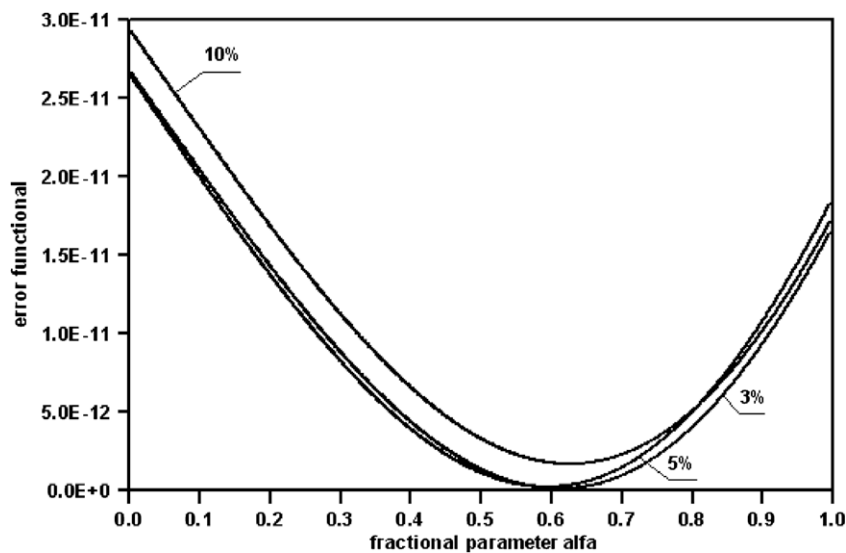


Fig. 17. Error functional  $\tilde{J}_M$  of the fractional Maxwell model versus the  $\alpha$  parameter for artificial data with noise intensities of 3%, 5% and 10%.

tice that the relative errors of values of  $\alpha$ ,  $k$  and  $c$  parameters are of the order of noises.

The third-kind method is also applied to the artificial experimental data. The following results are obtained:  $\alpha = 0.610$ ,  $k = 2,84,543.0$  N/m,  $c = 68,096.0$  Ns/m when 3% noises are randomly introduced to artificial data. The results of calculations performed for different noise levels are shown in Fig. 16. Additionally, in Fig. 17 the plot functional  $\tilde{J}_M$  (given by relationship (62)) of the fractional Maxwell model versus the parameter  $\alpha$  is presented for three levels of noises. In the range of values of interest of the parameter  $\alpha$  we have one minimum of the functional. Very similar results to those presented above are obtained using the second-kind method. Moreover, a similar plot to the one presented in Fig. 17 is obtained for the fractional Kelvin–Voigt model.

The results of calculations performed for artificial data showed that if the noise levels are not too high then all of the suggested

methods of parameters identification are not sensitive to the noises. Errors in the values of the parameters obtained in the identification procedures are of the order of the noise levels.

The next step is to apply the identification procedure to real experimental data. The experimental data presented by Makris and Constantinou [17] are chosen and used in this example. In their investigations, Makris and Constantinou were using a damper manufactured by GERB Schwingungsisolierungen GmbH & Co. KG. The following values of parameters of the fractional Maxwell model are determined:  $\alpha = 0.77$ ,  $k = 503.350$  kN/m,  $c = 13.823$  kNs/m. In Figs. 18 and 19 a comparison of the experimental and approximated storage modulus  $K'$  and the loss modulus  $K''$  is presented. The values of  $K'$  and  $K''$  resulting from the identification procedure are calculated from relationships (12) and (13). The presented model works satisfactorily. The identification procedure of the parameters of the fractional Maxwell model is simple, well applicable and efficient.

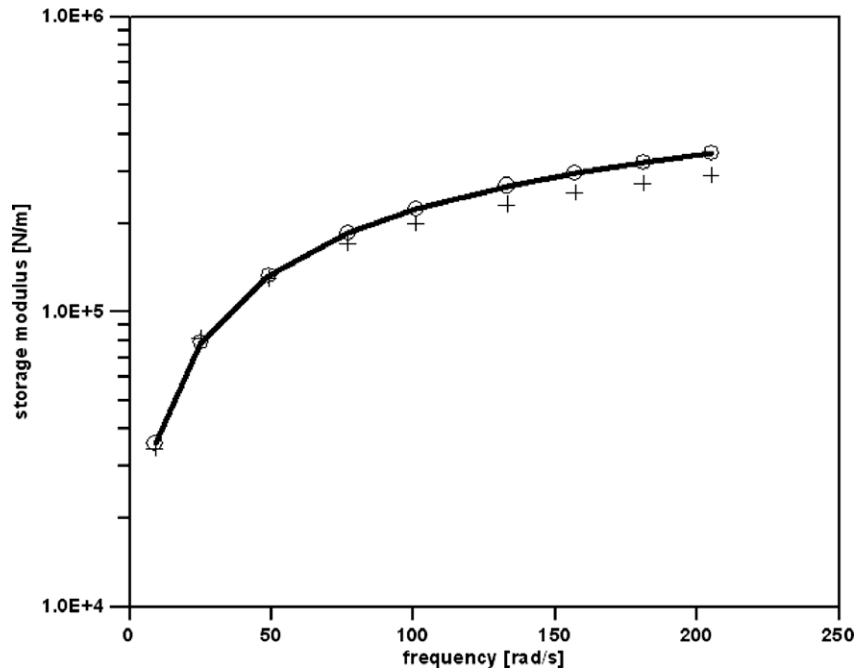


Fig. 18. Storage modulus – fluid damper.

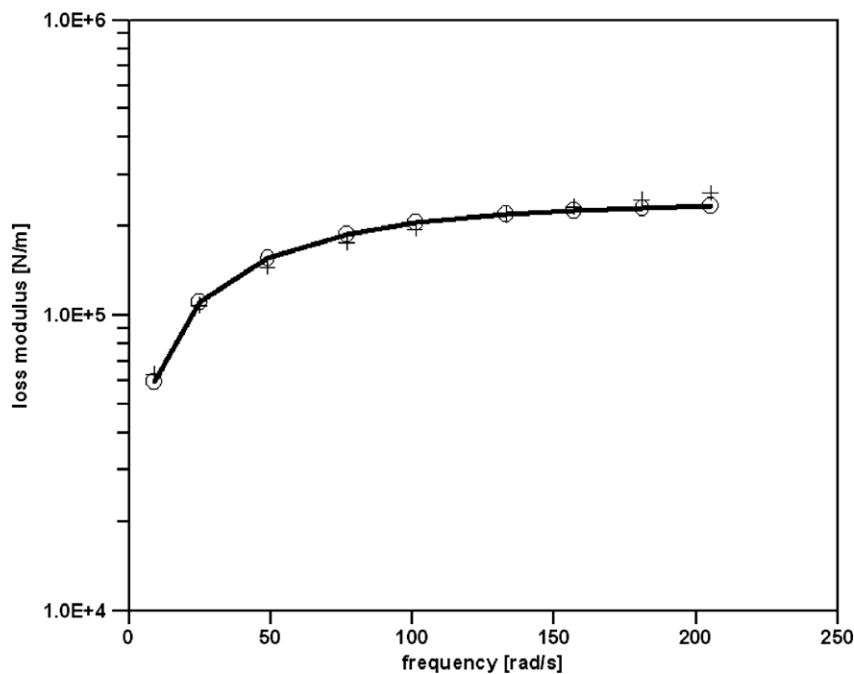


Fig. 19. Loss modulus – fluid damper.

## 7. Concluding remarks

A family of parameters identification methods for the Kelvin–Voigt and the Maxwell fractional models are proposed in the paper. Three kinds of identification methods are suggested to determine three parameters of the fractional Kelvin–Voigt model and the fractional Maxwell model. Each identification procedure consists of two main steps. In the first step, for the given frequencies of excitation, experimentally obtained data are approximated by simple harmonic functions while model parameters are determined in the second stage of the identification procedure. The parameters

of fractional models are determined using results from dynamical tests. The suggested identification methods differ substantially in comparison with previously proposed method. Rather than using the experimentally obtained complex modulus, the discussed methods directly utilize the measured steady state responses of damper. The methods could be also used when data are available only from a narrow range of excitation frequency. The results of calculation show that the proposed methods are not sensitive to the measurement noises and, therefore, it is not necessary to use regularization techniques. Similar calculation efforts are needed when each of the presented methods are used to identify the dam-

per parameters and the existing differences between the discussed methods have no significant influence of the effectiveness of the methods and on results of identification. All of the proposed identification procedures are simple, well applicable and efficient. Moreover, hysteresis loop equations are derived for both models. Some properties of the hysteresis curves are used to develop one of the identification procedures. The validity and effectiveness of the identification procedures have been successfully tested using both artificially generated and real experimental data. It was found that they are real VE dampers to which this model can be fitted with a satisfactory accuracy.

**Acknowledgments**

The authors wish to acknowledge the financial support received from the Poznan University of Technology (Grant No. DS 11-018/08) in connection with this work. The authors would like to express their appreciation to the reviewers for their valuable suggestions.

**Appendix A. Approximation of experimental data by trigonometric functions**

In this Appendix A we assume that, during the experimental tests, two output functions  $u_e(t)$  (function of force in a time domain) and  $q_e(t)$  (function of displacement in a time domain) which represent the steady state behavior of damper were obtained. Both functions could be approximated using simple trigonometric functions, as described below. Two procedures of the parameters identification based on time series data are presented in this Subsection.

Experimentally measured displacements of the damper are approximated using the function:

$$\tilde{q}(t) = \tilde{q}_c \cos \lambda t + \tilde{q}_s \sin \lambda t. \tag{A1}$$

Using the least-square method, parameters  $\tilde{q}_c$  and  $\tilde{q}_s$  of function (A1) are determined. This method requires minimization of the following functional:

$$J_1(\tilde{q}_c, \tilde{q}_s) = \frac{1}{t_2 - t_1} \int_{t_1}^{t_2} [q_e(t) - \tilde{q}(t)]^2 dt, \tag{A2}$$

where the symbols  $t_1$  and  $t_2$  denote the beginning and the end of the time range in which the damper's displacements were measured. Part of the measuring results related to steady state vibration are used as data in this identification procedure. From the stationary conditions of the functional (A2), the following system of equations with respect to parameters  $\tilde{q}_c$  and  $\tilde{q}_s$  are received:

$$I_{cc}\tilde{q}_c + I_{sc}\tilde{q}_s = I_{cq}, \quad I_{sc}\tilde{q}_c + I_{ss}\tilde{q}_s = I_{sq}, \tag{A3}$$

where

$$I_{cc} = \int_{t_1}^{t_2} \cos^2 \lambda t dt, \quad I_{ss} = \int_{t_1}^{t_2} \sin^2 \lambda t dt, \quad I_{cs} = I_{sc} = \int_{t_1}^{t_2} \sin \lambda t \cos \lambda t dt, \tag{A4}$$

$$I_{cq} = \int_{t_1}^{t_2} q_e(t) \cos \lambda t dt, \quad I_{sq} = \int_{t_1}^{t_2} q_e(t) \sin \lambda t dt. \tag{A5}$$

In a similar way the experimentally measured damper force is approximated using the following harmonic function:

$$\tilde{u}(t) = \tilde{u}_c \cos \lambda t + \tilde{u}_s \sin \lambda t. \tag{A6}$$

The parameters  $\tilde{u}_c$  and  $\tilde{u}_s$  are determined with the help of the last-square method. The functional and the system of equations with respect to  $\tilde{u}_c$  and  $\tilde{u}_s$  are:

$$J_2(\tilde{u}_c, \tilde{u}_s) = \frac{1}{t_2 - t_1} \int_{t_1}^{t_2} [u_e(t) - \tilde{u}(t)]^2 dt, \tag{A7}$$

$$I_{cc}\tilde{u}_c + I_{sc}\tilde{u}_s = I_{cu}, \quad I_{sc}\tilde{u}_c + I_{ss}\tilde{u}_s = I_{su}, \tag{A8}$$

where  $I_{cc}$ ,  $I_{ss}$  and  $I_{cs} = I_{sc}$  are given by relationships (A4). Moreover,

$$I_{cu} = \int_{t_1}^{t_2} u_e(t) \cos \lambda t dt, \quad I_{su} = \int_{t_1}^{t_2} u_e(t) \sin \lambda t dt. \tag{A9}$$

**References**

- [1] Christopoulos C, Filiatrault A. Principles of passive supplemental damping and seismic isolation. Pavia, Italy: IUSS Press; 2006.
- [2] Singh MP, Moreschi LM. Optimal placement of dampers for passive response control. Earthquake Eng Struct Dyn 2002;31:955–76.
- [3] Shukla AK, Datta TK. Optimal use of viscoelastic dampers in building frames for seismic force. J Struct Eng 1999;125:401–9.
- [4] Park SW. Analytical modeling of viscoelastic dampers for structural and vibration control. Int J Solids Struct 2001;38:8065–92.
- [5] Palmeri A, Ricciardelli F, De Luca A, Muscolino G. State space formulation for linear viscoelastic dynamic systems with memory. J Eng Mech 2003;129:715–24.
- [6] Singh MP, Chang TS. Seismic analysis of structures with viscoelastic dampers. J Eng Mech 2009;135:571–80.
- [7] Chang TS, Singh MP. Mechanical model parameters for viscoelastic dampers. J Eng Mech 2009;135:581–4.
- [8] Gerlach S, Matzenmiller A. Comparison of numerical methods for identification of viscoelastic line spectra from static test data. Int J Numer Meth Eng 2005;63:428–54.
- [9] Syed Mustapha SMFD, Philips TN. A dynamic nonlinear regression method for the determination of the discrete relaxation spectrum. J Phys D 2000;33:1219–29.
- [10] Pritz T. Analysis of four-parameter fractional derivative model of real solid materials. J Sound Vib 1996;195(1):103–15.
- [11] Atanackovic TM. A modified Zener model of a viscoelastic body. Continuum Mech Thermodyn 2002;14:137–48.
- [12] Song DY, Jiang TQ. Study on the constitutive equation with fractional derivative for the viscoelastic fluids – modified Jeffreys model and its application. Rheol Acta 1998;37(5):512–7.
- [13] Pritz T. Five-parameter fractional derivative model for polymeric damping materials. J Sound Vib 2003;265:935–52.
- [14] Bagley RL, Torvik PJ. Fractional calculus – a different approach to the analysis of viscoelastically damped structures. AIAA J 1989;27:1412–7.
- [15] Schmidt A, Gaul L. Finite element formulation of viscoelastic constitutive equations using fractional time derivatives. J Nonlinear Dyn 2002;29:37–55.
- [16] Aprile A, Inaudi JA, Kelly JM. Evolutionary model of viscoelastic dampers for structural applications. J Eng Mech 1997;123:551–60.
- [17] Makris N, Constantinou MC. Fractional-derivative Maxwell model for viscous dampers. J Struct Eng 1991;117:2708–24.
- [18] Honerkamp J. Ill-posed problem in rheology. Rheol Acta 1989;28:363–71.
- [19] Hansen S. Estimation of the relaxation spectrum from dynamic experiments using Bayesian analysis and a new regularization constraint. Rheol Acta 2007;47:169–78.
- [20] Beda T, Chevalier Y. New method for identifying rheological parameter for fractional derivative modeling of viscoelastic behavior. Mech Time-Depend Mater 2004;8:105–18.
- [21] Gaul L, Schmidt A. Parameter identification and FE implementation of a viscoelastic constitutive equation using fractional derivatives. PAMM (Proc Appl Math Mech) 2002;1(1):153–4.
- [22] Galucio AC, Deu JF, Ohayon R. Finite element formulation of viscoelastic sandwich beams using fractional derivative operators. Comput Mech 2004;33:282–91.
- [23] Castello DA, Rochinha FA, Roitman N, Magulga C. Modelling and identification of viscoelastic materials by means of a time domain technique. In: Proceedings of sixth world congress of structural and multidisciplinary optimization, Rio de Janeiro, Brazil; 30 May–03 June. p. 1–10.
- [24] Matsagar VA, Jangid RS. Viscoelastic damper connected to adjacent structures involving seismic isolation. J Civil Eng Manage 2005;11:309–22.
- [25] Lee SH, Son DI, Kim J, Min KW. Optimal design of viscoelastic dampers using eigenvalue assignment. Earthquake Eng Struct Dyn 2004;33:521–42.
- [26] Park JH, Kim J, Min KW. Optimal design of added viscoelastic dampers and supporting braces. Earthquake Eng Struct Dyn 2004;33:465–84.
- [27] Singh MP, Verma NP, Moreschi LM. Seismic analysis and design with Maxwell dampers. J Eng Mech 2003;129:273–82.
- [28] Hatada T, Kobori T, Ishida M, Niwa N. Dynamic analysis of structures with Maxwell model. Earthquake Eng Struct Dyn 2000;29:159–76.
- [29] Makris N, Zhang J. Time-domain viscoelastic analysis of earth structures. Earthquake Eng Struct Dyn 2000;29:745–68.
- [30] Spanos PD, Tsavachidis S. Deterministic and stochastic analyses of a nonlinear system with a Biot visco-elastic element. Earthquake Eng Struct Dyn 2001;30:595–612.

- [31] Adhikari S. Dynamics of non viscously damped linear systems. *J Eng Mech* 2002;128:328–39.
- [32] Papoulia KD, Panoskaltis VP, Korovajchuk I, Kurup NV. Rheological representation of fractional derivative models in linear viscoelasticity. *Rheol Acta*; in press.
- [33] Yin Y, Zhu KQ. Oscillating flow of a viscoelastic fluid in a pipe with the fractional Maxwell model. *Appl Math Comput* 2006;173:231–42.
- [34] Podlubny I. *Fractional differential equations*. Academic Press; 1999.
- [35] Lion A. Thermomechanically consistent formulations of the standard linear solid using fractional derivatives. *Arch Mech* 2001;53:253–73.
- [36] Zhu XQ, Law SS. Orthogonal function in moving loads identification on a multi-span bridge. *J Sound Vib* 2001;245:329–45.
- [37] Eldred LB, Baker WP, Palazotto AN. Kelvin–Voigt vs fractional derivative model as constitutive relations for viscoelastic materials. *AIAA J* 1995;33:547–50.
- [38] Soula M, Vinh T, Chevalier Y. Transient responses of polymers and elastomers deduced from harmonic responses. *J Sound Vib* 1997;205:185–203.
- [39] Kim SY, Lee DH. Identification of fractional-derivative-model parameters of viscoelastic materials from measured FRF's. *J Sound Vib* 2009;324:570–86.
- [40] Makris N. Complex-parameter Kelvin model for elastic foundations. *Earthquake Eng Struct Dyn* 1994;23:251–64.
- [41] Vasques CMA, Moreira RAS, Rodrigues JD. Experimental identification of GHM and ADF parameters for viscoelastic damping modeling. In: Mota Soares CA et al., editors. *Proceedings of the III European conference on computational mechanics. Solids, structures and coupled problems in engineering*, Lisbon, Portugal; 5–8 June 2008. p. 1–25.
- [42] Gerlach S, Matzenmiller A. On parameter identification for material and microstructural properties. *GAMM-Mitt* 2007;30:481–505.